17th World Conference on Earthquake Engineering, 17WCEE
Sendai, Japan- September13th to 18th 2020

IN-PLANE SEISMIC PERFORMANCE OF MASONRY INFILLED RC FRAME WITH AND WITHOUT FERRO-CEMENT OVERLAY

F. Zahura[(1)], D. Sen[(2)] , R. Sabrin[(3)], A. Das[(4)], M. Uddin[(5)], Z. Tafheem[(6)], F. Khanam[(7)], H. Alwashali[(8)], M. Maeda[(9)]

[(1)]*Associate Professor, Ahsanullah University of Science and Technology, Bangladesh,fatema1777@gmail.com*
[(2)]*PhD student, Tohoku University, Japan, dsendip@rcl.archi.tohoku.ac.jp*
[(3)]*Assistant Professor,Ahsanullah University of Science and Technology, Bangladesh,rishathsabrin@gmail.com*
[(4)]*Junior Research Consultant, House Building Research Institute, Bangladesh,anikdas503@gmail.com*
[(5)]*Junior Research Consultant,, House Building Research Institute, Bangladesh,jshaon@gmail.com*
[(6)]*PhD student,Tohoku University, Japan,zasiah@rcl.archi.tohoku.ac.jp*
[(7)]*Junior Research Consultant, House Building Research Institute, Bangladesh,khanamfarjana2@gmail.com*
[(8)]*Assistant Professor,Tohoku University, Japan,hamood@rcl.archi.tohoku.ac.jp*
[(9)]*Professor,Tohoku University, Japanmaeda@rcl.archi.tohoku.ac.jp*

Abstract

Several low performance buildings are located in developing countries of earthquake prone region, like Bangladesh, which poses threat to life safety and damage of property during an earthquake. Damage of RC buildings in Nepal earthquake (2015) can be regarded as an evidence of the potential risk. In this context an appropriate (reliable, effective and low cost) retrofitting scheme is a challenging issue for the existing low performance RC buildings in Bangladesh. In general, the basic characteristics of RC buildings of Bangladesh are the presence of clay brick masonry as partition wall because masonry is relatively cheap. This non-structural masonry can be treated as a structural part using some retrofitting to get an enhanced lateral performance under seismic load. In this study, wire mesh embedded mortar layer that is known as Ferro-cement, is applied on masonry infilled RC frame as an easy to apply retrofitting technique.

The present study deals with evaluation of seismic performance of two half-scaled single-story, single-bay masonry infilled RC frame with and without Ferro-cement retrofitting. The primary objective of this study is to investigate the seismic performance of Ferro-cement laminated infilled masonry under cyclic lateral load. It is also aimed to estimate the lateral capacity of the test specimens based on the failure mode observed in the experimental program. Common design practice and locally available materials were selected for the test specimens to represent typical RC building frames that have been constructed earlier in Bangladesh.

Based on the experimental investigation of two half scaled RC frame as mentioned earlier, lateral strength, lateral stiffness, ductility, energy dissipation and failure modes is presented in this paper. The experimental results exhibited that lateral load carrying capacity of the strengthened specimen approximately raised by 80% in positive cycle and 19% in negative cycle with the reduction of ductility. In different load cycles, changes in crack pattern and propagation of cracks were also monitored to investigate the failure mechanism. Based on the experimentally observed failure mechanism, theoretical prediction model for the Ferro-cementstrengthened masonry infilled RC frame specimen were developed and verified with the test results with reasonable accuracy.

Keywords: Retrofitting; Masonry infill walls; Ferro-cement; RC frame; Lateral stiffness.

1. Introduction

Risk of old buildings situated in earthquake prone areas triggered interest among researchers to retrofit the vulnerable buildings. Major concern plumes around the fact that the buildings which are situated in developing countries like Bangladesh require low cost strengthening technique. Since, RC buildings in developing countries like Bangladesh contain clay brick masonry partition wall, strengthening of existing infill masonry by ferro-cement could be a low cost solution.Generally,unreinforced masonry infill improves in plane lateral strength and stiffness and this contribution is not considered in the design procedure. However, unreinforced masonry wall is brittle in nature and susceptible to failure under small lateral drift. Lamination of ferro-cement improves the strength of masonry wall and can contribute to the total lateral strength of the RC frame. Hence, consideration of masonry wall laminated with ferro-cement as a structural element could fairly optimize the demand of strength up gradation and cost effective technique. Amongst the various features related with strengthening, enhancement of lateral strength of vulnerable old buildings of developing countries is the prime concern of this study. In this study, as a part of JST sponsored SATREPS-TSUIB project in Bangladesh (https://www.satreps-tsuib.net/), authors are trying to develop an effective way to retrofit existing infill masonry with ferro-cement lamination as a low cost and less labour intensive strengthening method. In this regard research works carried out by several researchers were studied. Half scaled masonry infilled RC frames with and without ferro-cement strengthening were tested experimentally by Kaya et al. [1], Seki et al. [2], Demirel et al. [3], Altin et al. [4], Calvi and Bolognini [5], Alcocer et al [6], Žarnić and Tomaževič [7] and Sen et al. [8]. Most of them provided connections between wire mesh and RC frame. However, connection with RC frame is difficult in Bangladesh due to unavailability of structural drawing for old structures of concern. Owing to this reason connection with RC frame is has not been utilized in this study. This study aims to experimentally investigate the lateral behavior of masonry infilled RC frames, with and without ferro-cement lamination subjected to lateral cyclic load. The second objective is to evaluate the lateral capacities of un-strengthened and strengthened specimens. The established lateral capacity evaluation method of un-strengthened specimen is verified and the lateral capacity of the ferro-cement laminated specimens, which is absent in the previous research works, is also proposed based on the failure mode observed in the experimental program.

2. Experimental program

2.1 Specimen Details

In this study two half scaled masonry infilled RC frames, with and without Ferro-cement strengthening were considered. Among the two specimens, masonry infilled RC frame was considered as control specimen and identified as IM. Another masonry infilled RC frame was strengthened using ferro-cement lamination and designated as IM-FC. Common design practice and locally available materials were selected for the test specimens to represent typical RC building frames that have been constructed earlier in Bangladesh. Initially, two half scaled RC frames were constructed. Then both RC frames were filled with 115mm thick masonry infill using burnt clay brick having 14 MPa compressive stress. Dimensions of brick sample and the control specimen (IM) along with cross section of beams and columns were depicted in Fig.1. Information of the embedded longitudinal and shear reinforcements are also shown in Fig.1. After seven days of construction of infill masonry, 10mm mortar was applied on both surfaces of one masonry infilled RC frame designated as IM-FC.Fig.2 portrays the physical appearance of the ferro-cement laminated strengthened specimen IM-FC. After that, square wire mesh having 1 mm diameter was mounted on both faces of the wall using 38mm long nails. Enlarged view of the attachment of wire mesh is shown in Fig.3. Top edge of the nails were bend to form hook for achieving better bonding of the wire mesh with mortar into which it is embedded. Layer of epoxy surrounding the nails has been used for bonding between nails and masonry. Finally, another 10mm mortar was applied on the both faces of the wall. The total thickness of ferro-cement mortar on each masonry surface was 20mm. Details of all specimens are summarized in Table 1.

Table 1 - Details of all specimens

Specimen	RC column		Masonry	Ferro-cement			
	Dimension *mm*	Main Reinforcement	Thickness t_{mas} (mm)	Thickness t_{FC} (mm)	Wire diameter φ_{wm} (mm)	Wires pacing s (mm)	Number of mesh layers
IM	165x165	4-12mmφ	115	-	-	-	-
IM-FC				20	1.0	7	1

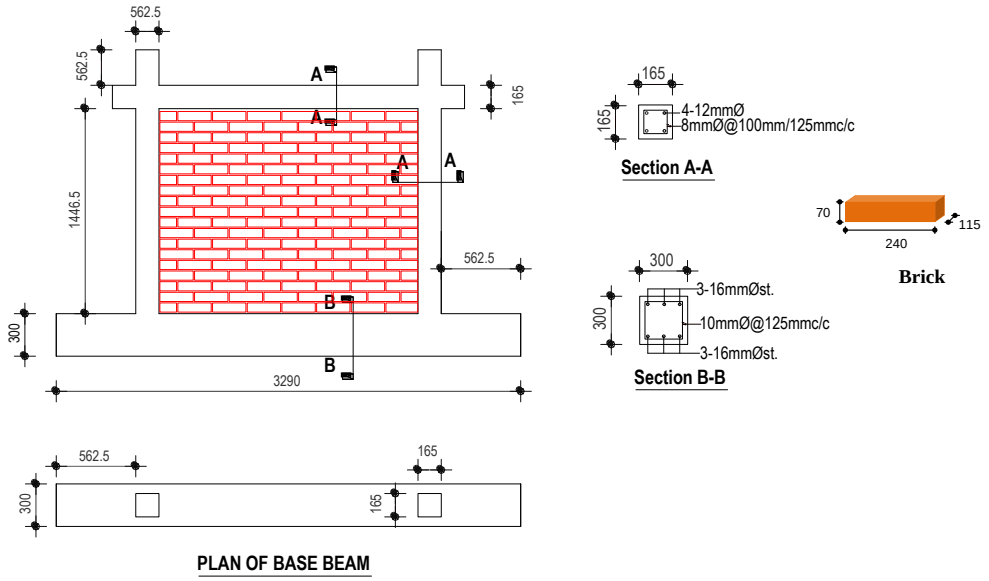

Fig. 1– Geometry of control infilled masonry specimen (IM) [All dimensions are in mm]

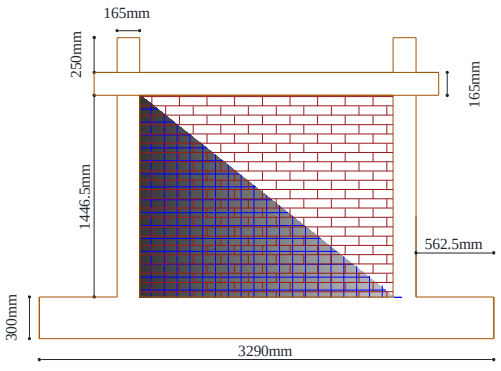

Fig. 2 – Geometry of ferro-cement laminated strengthened specimen (IM-FC)

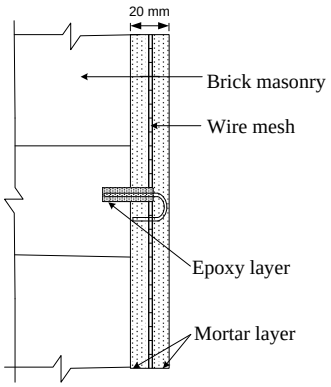

Fig. 3 – Enlarged view of wire mesh attachment using nail

2.2 Material properties

Same mix design was adopted for manufacturing of concrete for both RC frame specimens and the concrete strength was about 18MPa.For masonry construction, 1:2:4 mix ratio with 0.4 w/c ratio was adopted for the joint mortar of both specimens. 50 mm cube mortar specimens were tested for compressive strength of mortar. ASTM C1314 [9]is followed for the computation of masonry prism compressive strength. The wire mesh has been tested as per ACI 549[10]. Mechanical properties of the concrete, masonry, mortar and wire mesh used are presented in Table 2. Nominal yield strength of long reinforcement (φ-12mm) and shear reinforcement (φ-8mm) were 415 MPa and 275 MPa, respectively.

Table 2 – Properties of materials used in the experimental study

Specimen	Concrete	Masonry		Mortar	Wire Mesh	Brick
	Compressive Strength	Compressive strength	Sliding strength	Compressive strength	Ultimate tensile strength	Compressive strength
	MPa	MPa	MPa	MPa	MPa	MPa
IM	18.85	5.54	0.48	10.32	-	14
IM-FC					281	

2.3Instrumentation and loading protocol

Schematic diagram of the experimental setup is shown in Fig.4. Hydraulic jack was used to apply static cyclic load resembling seismic effect. Each cycle of the lateral load consisted of push and pull with loading and unloading sequence. Lateral story drift applied in different cycles were 0.05, 0.1, 0.2, 0.4, 0.6, 0.8, 1.0, 1.5, and 2.0 %. Lateral story drift is defined as the ratio of the top lateral displacement, measured at the center of column by using LVDTs shown in Fig. 4, to the height of column is defined as lateral drift. As stated earlier in plane behavior of masonry infilled frame is the concern of this study, out of plane movement was monitored using LVDTs attached at the same place of story displacement LVDTs.

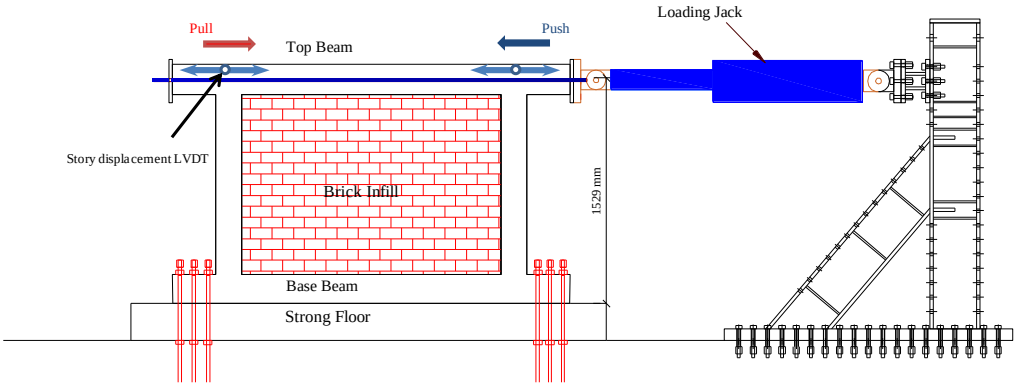

Fig. 4– Schematic diagram of experimental setup

3. Experimental results

3.1 Cyclic behavior under lateral load

Hysteretic response of control infilled masonry specimen (IM) and ferro-cement laminated strengthened specimen (IM-FC) is depicted in Fig.5 and Fig.6 respectively. Behavior of the hysteretic curves is described in the following sub-sections. It is to be noted that the push and pull phase have been considered synonymously as positive and negative direction for the discussion.

3.1 .1 Infilled masonry specimen (IM)

At first, flexural crack appears at the bottom of tension column during the push phase of 0.05% lateral drift. Then, the flexural cracks opened along with formation of additional flexural cracks up to mid height of the tension column. At 0.2% story drift, stair stepped diagonal crack formed on the infill masonry and opened about 3mm at 0.4% story drift. At 0.6% story drift, bed joint cracks formed on infill masonry revealing weak point near the mortar joints of brick masonry. At 1% story drift of push phase, the masonry infilled RC frame exhibited maximum lateral resistance of 98 kN. In pull phase, the maximum lateral resistance was -108kN at

about 1.5% story drift. The specimen was pulled up to -5% for better understanding the failure mechanism. The final cracking pattern and damaged specimen at -5% story drift, is shown in Fig.7 and Fig.8. As illustrated in Fig.8 the hinges at tension column were formed at the mid-height and at the top indicating short column effect due to the sliding of the infill masonry.

3.1 .2 Ferro-cement laminated strengthened specimen (IM-FC)

At initial stage, flexural cracks on tension column appeared up to mid height of the column at 0.05% story drift. Several shear cracks also occurred above the mid-height of tension column at the same story drift. At 0.1% story drift separation of infill from tension column occurred to mid height and gradually increased with the increase of story drift. At 0.2% story drift, cracks appeared at the upper joint of the FC laminated masonry and top beam soffit which indicates the sliding at the top construction joint. Following the sliding at the top joint, tension column exhibited shear cracking at 0.4% story drift. At 0.6% story drift, the specimen IM-FC exhibited maximum lateral resistance of 176 kN associated with the extension of shear cracks on the top of tension column and sliding at the top joint. Delamination of FC layer at the loading corner has also been evident. In pull phase, the maximum capacity was about -108kN at about -0.4% story drift. The large difference between the maximum capacity in push and pull phase could be attributed to the bond failure of the top interface in push phase; resulting absence of bond strength at the pull phase. After that, the sliding increased at the top which lead to direct shear failure or punching shear failure of the top of tension column, as shown in Fig. 10, at 1.5% story drift. As capacity in the pull phase degrades to approximately 17% at -1.5% story drift, loading was ceased at this phase owing to the safety concern. Final cracking pattern and damaged specimen of IM-FC is shown in Fig.9 and Fig.10. It is to be noted that there was no trace of cracks appeared on the surface of the FC, except the delamination and cracks at the construction joints.

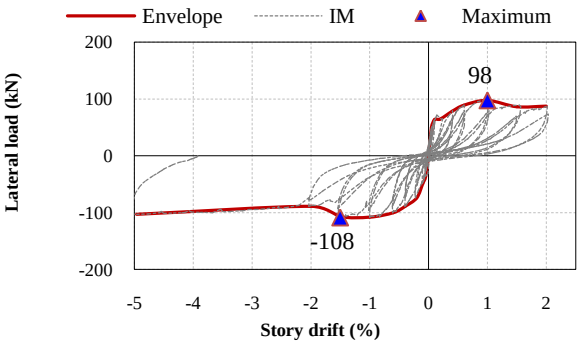

Fig. 5 – Lateral load vs story drift curve for control infilled masonry specimen (IM)

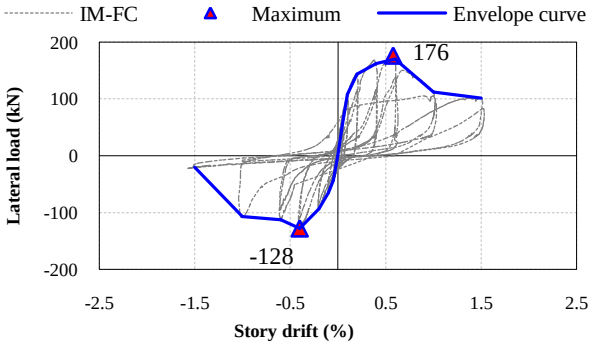

Fig. 6 – Lateral load vs story drift curve for Ferro-cement Laminated Strengthened specimen (IM-FC)

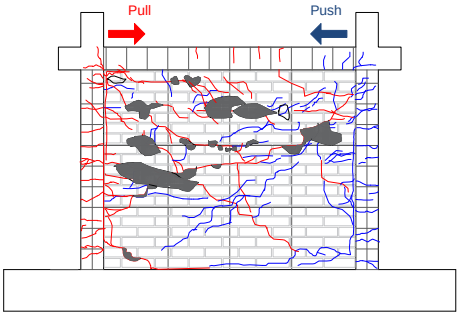

Fig. 7 – Cracking pattern of control specimen (IM) after -5% story drift

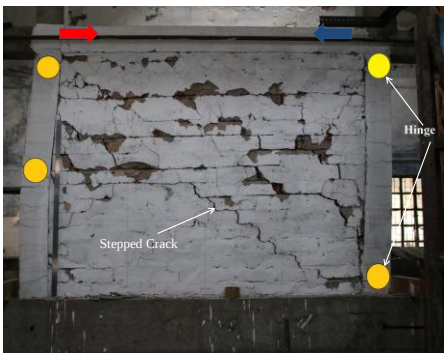

Fig. 8 – Damaged specimen at -5% story drift of control specimen (IM)

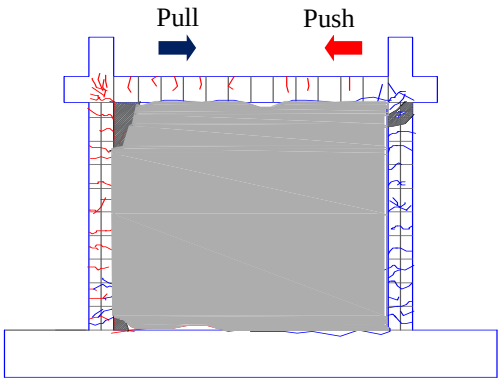

Fig. 9 – Cracking pattern of Ferro-cement Laminated specimen (IM-FC)

Fig. 10 – Final damage of Ferro-cement Laminated specimen (IM-FC)

4. Discussion on Experimental Results

4.1 Comparison of lateral capacities

For the comparison of lateral behavior, experimental backbone curves of the specimens are shown in Fig.11. The masonry infilled RC frame (IM) showed maximum lateral resistance of 98kN and -108 kN at 1.0% and -1.5% story drift, respectively. The lateral capacity did not degrade much which is thought to be due to the sliding of infill masonry. Moreover, FC laminated masonry infilled RC frame (IM-FC) showed maximum lateral resistance of 176kN and -128kN at 0.6% and -0.4% story drift, respectively, which is in average about 1.5 times greater than masonry infilled RC frame's (IM) lateral capacity. However, the failure mechanisms were completely different for the specimen IM and IM-FC.

As discussed in the earlier section, the main load transfer mechanism of the specimen IM was the sliding of infill masonry, whereas in specimen IM-FC, load transfer mechanism was the sliding at top construction joint following tension column punching. In specimen IM-FC, after bond failure at the top construction joint, lateral capacity dropped about 44% in the push direction.

In case of FC laminated masonry infilled RC frame, the peak resistance came at lower story drift that can be attributed to the higher stiffness and strength of the FC laminated masonry infill compared to relatively softer infill masonry. Therefore, from this experimental observation, it can be concluded that Ferro-cement can be used to strengthen infill masonry when strength upgradation is the primary concern rather than both strength and ductility.

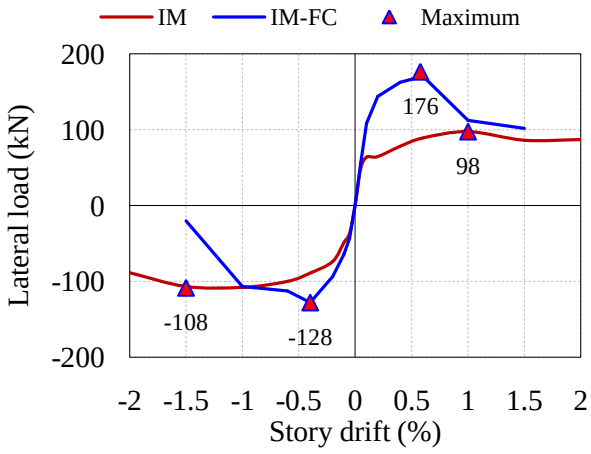

Fig. 11 – Comparison of experimental envelope curves of Specimen IM and IM-FC

4.2 Parameters of hysteretic curve

Behavior of structures under seismic load depends upon the parameters of hysteretic curve of the lateral-load resisting system. As lateral-load resisting system should be designed in order to provide adequate energy dissipation mechanisms via plastic deformation, parameters such stiffness degradation and pinching of hysteretic response of structures are vital.

Pinching, stiffness degradation and load degradation are some parameters to describe the hysteretic response of structure under cyclic load. Pinching is the phenomenon which usually is the result of crack closure, alternatively, due to occurrence of pinching, hysteretic loops becomes narrower in the middle and wider at the ends. RCC structures under reverse cyclic load exhibits gradual loss of lateral stiffness which is known as stiffness degradation represented by stiffness degradation coefficient, d. Calculated value of stiffness degradation coefficient, d for IM and IM-FC obtained from Fig.5 and Fig.6 is 0.98 and 0.96 respectively. A lower value of d value for the case of IM-FC system than that of IM indicates a lesser value of ductility in terms of story drift, as also confirmed from the hysteretic curve. It is also observed from the hysteretic curve that high pinching behavior occurs in case of IM specimen whereas low pinching behavior is the case for IM-FC.

4.3 Energy dissipation and stiffness degradation

Since energy dissipation is an indirect measure of ductile or brittle behavior, therefore the average cumulative energy dissipation at different story drifts of both specimens are shown in Fig.12.It is evident that the specimen strengthened with ferro-cement (IM-FC) dissipated about 6.5 times energy than the specimen without strengthening (IM) which indicates relatively ductile behavior in terms of energy dissipation.

The stiffness degradation curves of specimens IM and IM-FC are shown in Fig.13. Initial stiffness calculated from the hysteretic curve of control specimen (IM) and FC strengthened specimen (IM-FC) are 65 kN/mm and 74.5 kN/mm, respectively. It is evident from Fig.13 that, the stiffness degradation for the FC strengthened specimen (IM-FC) is relatively gradual than the masonry infilled RC frame specimen (IM).

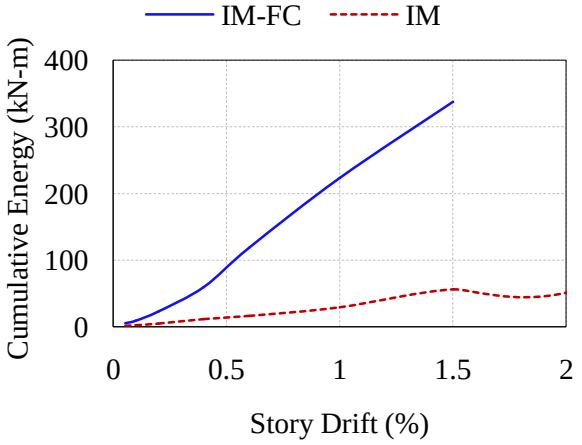

Fig. 12– Average cumulative energy dissipation of both specimens

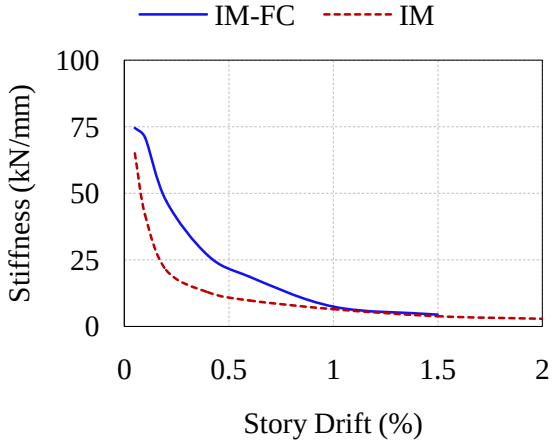

Fig. 13– Comparison of stiffness degradation of both specimens

5. Capacity evaluation of test specimens

The lateral capacity evaluation of un-strengthened and FC strengthened masonry infilled RC frame are discussed in this section. The overall backbone curve of the masonry infilled RC frame under lateral loading has been discussed and verified according to a simplified procedure proposed by Alwashali et al. [11]. On the other hand, the lateral capacity of FC strengthened masonry infilled RC frame has been proposed and verified in the following subsection.

5.1 Masonry infilled RC frame (IM)

A schematic backbone curve for the simplified procedure proposed by Alswashali et al. [11] is shown in Fig. 14. Backbone curve of masonry infilled RC frame consists of three main points namely cracking point, A, maximum point, B and residual point C, determination of each point is discussed in this sub-section.

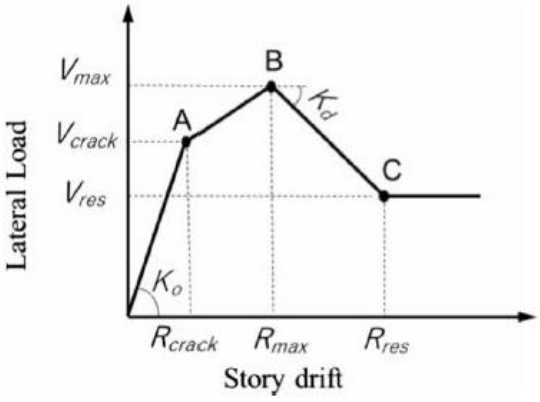

Fig. 14–Schematic backbone curve according to Alwashali et al. [11]

The initial stiffness (K_0) has been calculated as the summation of the stiffness of the RC frame (K_f) and infill masonry (K_m). The initial stiffness of RC frame and masonry was determined using Eq. (1) and (3).

$$K_f = 2\frac{12EI_c}{h_c^3}.\frac{12\rho+1}{12\rho+4} \text{ Where } \rho = \frac{\sum E_c I_b/l_b}{\sum E_c I_c/h_c} \quad (1)$$

$$K_m = \frac{E_m . W_{ef} . t_{inf} . cos^2\theta}{d_m} \quad (2)$$

Where, W_{ef} = Effective width of strut, $= 0.2d_m$ and d_m = Diagonal length of infill.

Point B indicates lateral capacity of masonry infilled RC frame (V_{max}).Lateral capacity of point B has been considered as the summation of bare RC frame capacity (V_f) and the contribution of the infill masonry (V_{mas}) as explained in Eq. (4). The lateral capacity of bare frame can be calculated as per JBDPA[12], using Eq. (5) and Eq. (6).

$$V_{max} = V_f + V_{mas} \quad (3)$$

$$V_f = 2 \text{ x } Q_{mu} \quad (4)$$

$$Q_{mu} = \frac{2M_u}{h_o} \quad (5)$$

where,Q_{mu}= lateral capacity of column at flexural yielding at top and bottom, M_u = ultimate moment capacities of column, and h_o = clear height of column.

In the study by Alwashali et al. [11], the lateral contribution of masonry infill is considered according to FEMA 306 [13]. The contribution of infill masonry (horizontal component of the diagonal strut capacity) is calculated from Eqs. (6) through (8);

$$V_{mas} = f_{m,90} W_s t_{mas} \quad (6)$$

$$W_s = 0.175(\lambda_1 h)^{-0.4} d_m \quad (7)$$

$$\lambda_1 = \sqrt[4]{\frac{E_{mas} * t_{mas} * sin 2\theta}{4E_c I_c h_o}} \quad (8)$$

Where W_{ef} is the equivalent strut width calculated using Eq. (6), t_{inf} is the infill thickness, E_w and E_c are the elasticity moduli of the infill wall and the concrete. H_{inf} and H are the net height of infill wall and the story height. θ is the arctan (h_{inf}/L_{inf}) (the inclination of the diagonal). I_c is the moment of inertia of the column, d_m is diagonal length of masonry infill,$f_{m,90}$is the expected prism compressive strength of masonry in horizontal direction, which may be set at 50% of the expected prism compressive strength in absence of experimental results.

Story drift at maximum lateral capacity V_{max} is $R_{max}$and is calculated byEq. (9)

$$R_{max}= \frac{\varepsilon_{peak} .d_m}{cos\theta}. \quad (9)$$

Where ε_{peak} is the masonry compression strain at maximum compression stress which can be found from masonry prism test. Value of ε_{peak} usually varies within the range between 0.002 and 0.004. In absence of data ε_{peak} can be calculated based on empirical equations of Kaushik et al. [14].

The cracking lateral strength, at point A, is taken as 0.7 V_{max} where cracking story drift (R_{crack}) can be calculated using initial stigffnessk$_0$. The residual capacity (V_{res}) corresponding to point C is the summation of contribution of frame and infill. Contribution of frame is same as previously calculated whereas contribution of masonry is taken as 30% of the capacity of infill. Slope of the degradation part is calculated from regression analysis of previously performed experimental data and is shown in the following equation:

$K_d = \eta . K_m$ where $\eta = \frac{0.08}{\beta^{0.75}}$ and β is the ratio of lateral strength of frame to masonry infill.

5.2 Ferro-cement laminated masonry infilled RC frame

Load transfer mechanism of FC strengthened masonry infilled RC frame after top construction joint failure and column punching is shown in Fig. 15. The total lateral capacity (Q) can be evaluated by Eq. (10).

$$Q = {}_{ps}Q_c + {}_{js}Q_w + {}_{f}Q_c \quad (10)$$

Where, ${}_{ps}Q_c$ = punching shear resistance of tension column, ${}_{js}Q_w$ = shear resistance at construction joint, and ${}_{f}Q_c$= flexural shear resistance of compression column.

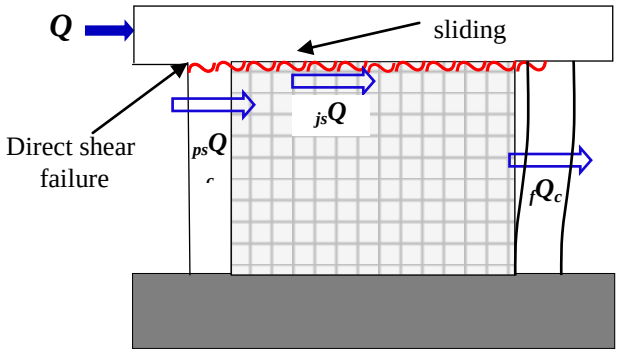

Fig. 15-Observed load transfer mechanism ofIM-FC

Punching shear capacity (${}_{ps}Q_c$) of tension column, and lateral capacity of compression column (${}_{f}Q_c$) of can be computed as per JBDPA 2001[12] using Eq. (11) and Eq. (12), respectively. The source of joint shear capacity (${}_{js}Q_w$) has been considered as the strength provided by masonry joint mortar and mortar of FC layer. Since, sliding occurred at the top construction joint, therefore at the peak strength shear capacity can be considered as shear strength (cohesion) of mortar at interface as suggested by Sen et al.[15]. The joint shear capacity can be evaluated from Eq. (13).

$$_{ps}Q_c = K_{\min}\tau_o bD \tag{11}$$

$$_{f}Q_c = \frac{2M_c}{h_o} \tag{12}$$

$$_{js}Q_w = \tau_{mas}\, l_w t_{mas} + \tau_{mor,FC}\, l_w n_s t_{FC} \tag{13}$$

where, K_{min} = 0.34/(0.52+a/D), a= shear span = D/3, τ_o = shear strength of tension column, b and D = width and depth of column, Mc= ultimate moment capacity of column, h_o= clear height of column, $_{js}Q_w$ = initial shear capacity at joint, τ_{mas}/$\tau_{mor,FC}$= shear strength (cohesion) of mortar in masonry joint and Ferro-cement, l_w = length of infill, t_{mas}/ t_{FC} = thickness of masonry wall and FC layer, n_s = number of FC surface. It is to be noted that cohesion capacity of mortar, for both masonry and FC layer, has been considered as $0.17\sqrt{f_{mor}}$, (f_{mor}=compressive strength of mortar), which has been recommended by Namaan 2000[16], and Mander and Nair 1994 [17] as shear strength of FC.

5.3 Comparison with experimental results

Comparison of evaluated capacities with experimental results of IM and IM-FCare shown in Fig. 16(a)-(b) and also reported in Table 3.

By comparing experimental and predicted backbone curve by Alwashali [11], as shown in Fig. 16(a), it is evident that the lateral behavior evaluation procedure of masonry infilled RC frame proposed by Alwashali [11]can predict the overall lateral behavior with good agreement. The calculated and experimental initial stiffness values are 65 kN/mm and 64 kN/mm, respectively. The calculated RC frame capacity is about 34kN and capacity of masonry is calculated as 58 kN, considering diagonal strut. Hence calculated capacity of IM specimen is 92 kN and is in good agreement with the experimental capacity which is 103 kN (average of push and pull direction). However diagonal compression failure of masonry, as suggested by FEMA 306 [13] and adopted by Alwashali et al. [11]was not the failure mode of experimental specimen IM. Damaged specimen of IM (Fig.8) reveals that sliding behavior occurred during the failure of the masonry specimen. Owing to this disparity in prediction of failure mechanism steeper post peak degradation happens in predicted backbone curve than the experimental curve.

For specimen IM-FC, the calculated RC frame capacity is about 94kN, considering punching failure and flexural hinge formation of tension and compression column, respectively. The computed joint sliding capacity is about 84kN. Hence, the calculated ultimate capacity is about 178kN. It is evident from Fig. 16(b) that, the calculated capacity (176 kN) agreed with the experimental lateral capacity in push direction with calculated to experimental lateral capacity ratio of 0.99. However, in pull direction calculated value (176 kN) overestimated the lateral capacity with calculated to experimental lateral capacity ratio of 1.37, which could be attributed to the bond failure of the top interface in push phase; resulting absence of bond strength at the pull phase.

Table 3-Calculated lateral capacities

Specimen	Experimental peak resistance (average of push and pull)	Calculated capacity
	kN	kN
IM	103	92
IM-FC	152	178

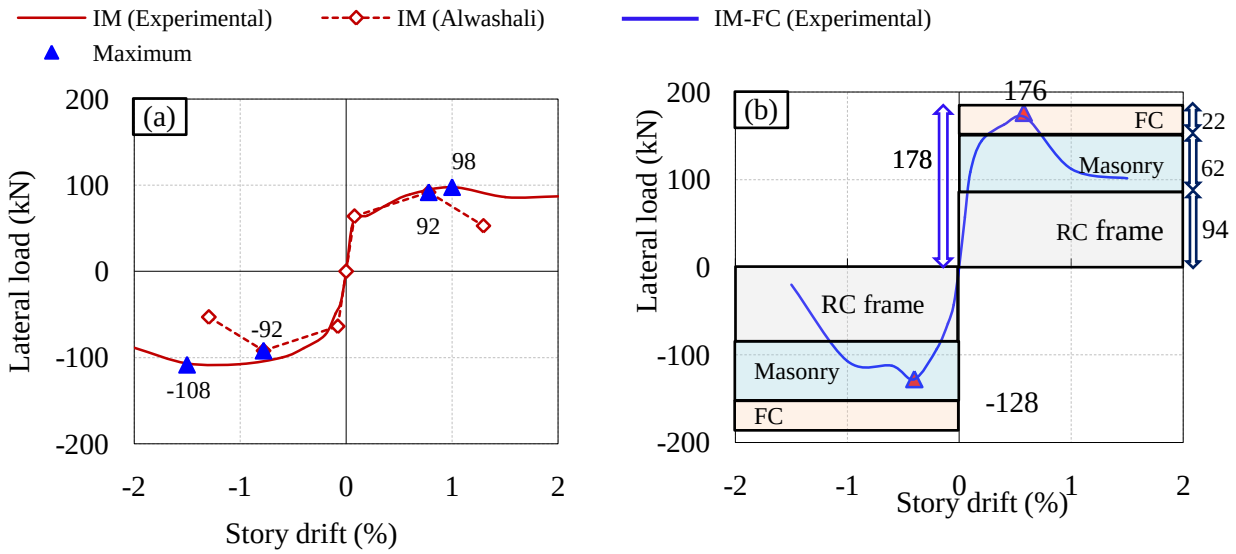

Fig. 16 -Comparison of evaluated capacities with experimental results of (a) IM and (b) IM-FC

5. Conclusions

Experimental study was carried out to investigate the behavior of masonry infilled frame strengthened with ferro-cement as an option of cheap and simple strengthening technique subjected to seismic load. Analysis of the results obtained from the experimental study in terms of parameters of hysteretic curve, initial stiffness, energy dissipation and failure mechanism. Seismic evaluation of the capacities of un-strengthened and FC strengthened specimens are also discussed. Following conclusions are drawn from this study:

- Ferro-cement lamination, using 0.14% wire mesh, on masonry infilled RC frame increased the lateral load carrying capacity about 50% when compared to masonry infilled RC frame. However, failure mode of un-strengthened and strengthened specimens was different i.e. sliding of infill masonry, and sliding at top construction joint following column punching, respectively.
- The overall behavior of masonry infilled RC frame as proposed by Alwashali [11]has been verified with the experimental program. Backbone curve until maximum strength could be simulated with good agreement; however, there was difference in the post peak of backbone curve, where the proposed model by Alwashali showed steeper strength degradation. This could be attributed to the sliding behavior due to weak mortar joints.
- The capacity evaluation of the observed failure mechanism i.e. top construction joint and column punching, of FC laminated masonry infilled RC frame has been proposed and verified with fare agreement having calculated to experimental lateral capacity ratio of 0.99 and 1.37 in push and pull direction, respectively.

7. Acknowledgement

This research is supported by SATREPS project "Technical Development to Upgrade Structural Integrity of Buildings in Densely Populated Urban Areas and its Strategic Implementation towards Resilient Cities (TSUIB)" (principle investigators: Prof. Yoshiaki Nakano, U. Tokyo and Mr. Mohammad Shamim Akhter, HBRI, Bangladesh). Authors also warmly acknowledge thehelp of Mr. Abdullah Al Hashib (AUST), Ms. Zannatul Alam (HBRI) and Ms. Maisha Maliha (Tohoku University)for their participation during specimen loading and material test.

6. References

[1] Kaya, F., Tekeli, H., and Anil, Ö., "Experimental behavior of strengthening of masonry infilled reinforced concrete frames by adding rebar ‐ reinforced stucco," *Structural Concrete*, vol. 19, pp. 1792-1805, 2018.

[2] Seki, M., Popa, V., Lozinca, E., Dutu, A., and Papurcu, A., "Experimental Study on Retrofit Technologies for RC Frames with Infilled Brick Masonry Walls in Developing Countries," in *16 European Conference on Earthquake Engineering (16ECEE), Thessaloniki, Greece, June*, 2018, pp. 18-21.

[3] Demirel, I., Yakut, A., Binici, B., and Canbay, E., "An Experimental Investigation of Infill Behaviour in RC Frames," in *Proceedings of the Tenth Pacific Conference on Earthquake Engineering Building an Earthquake-Resilient Pacific*, 2015, pp. 6-8.

[4] Altın, S., Anıl, Ö., Kopraman, Y., and Belgin, Ç., "Strengthening masonry infill walls with reinforced plaster," *Proceedings of the Institution of Civil Engineers-Structures and Buildings*, vol. 163, pp. 331-342, 2010.

[5] Calvi, G. M. and Bolognini, D., "Seismic response of reinforced concrete frames infilled with weakly reinforced masonry panels," *Journal of Earthquake Engineering*, vol. 5, pp. 153-185, 2001.

[6] Alcocer, S., Ruiz, J., Pineda, J., and Zepeda, J., "Retrofitting of confined masonry walls with welded wire mesh," in *Proceedings of the Eleventh World Conference on Earthquake Engineering*, 1996.

[7] Zarnic, R. and Tomazevic, M., "Study of the behavior of masonry infilled reinforced concrete frames subjected to seismic loading," in *Proc. 7th Intl. Brick Masonry Conf*, 1985.

[8] Sen, D., Torihata, Y., Alwashali, H., Islam, S., Tafheem, Z., and Maeda, M., "Investigation of the Ferro-cement laminated infilled masonry wall under cyclic lateral load."

[9] International, A., "ASTM C 1314–03b: Standard test method for compressive strength of masonry prisms," ed: ASTM International West Conshohocken, PA, 2003.

[10] Sakthivel, P., Ravichandran, A., and Alagumurthi, N., "An Experimental Study on Mesh-and-Fiber Reinforced Cementitious Composites," *Concrete Research Letters*, vol. 5, 2014.

[11] Alwashali, H., Torihata, Y., Jin, K., and Maeda, M., "Experimental observations on the in-plane behaviour of masonry wall infilled RC frames; focusing on deformation limits and backbone curve," *Bulletin of Earthquake Engineering*, vol. 16, pp. 1373-1397, 2018.

[12] Standard for seismic evaluation of existing concrete (2001):Japan Building Disaster Prevention Association.

[13] Basic procedures manual, *FEMA, Washington, DC, (*1998):Evaluation of earthquake damaged concrete and masonry wall buildings:

[14] Kaushik, H. B., Rai, D. C., and Jain, S. K., "Stress-strain characteristics of clay brick masonry under uniaxial compression," *Journal of materials in Civil Engineering*, vol. 19, pp. 728-739, 2007.

[15] Sen, D., Alwashali, H., Tafheem, Z., Islam, M.S., Maeda, M, Seki, M. , " Experimental investigation and capacity evaluation of ferro-cement laminated masonry infilled RC frame," *17th World Conference on Earthquake Engineering, Sendai, Japan*, 2020.

[16] Naaman, A. E., *Ferrocement and laminated cementitious composites* vol. 3000: Techno press Ann Arbor, 2000.

[17] Mander, J. and Nair, B., "Seismic resistance of brick-infilled steel frames with and without retrofit," *TMS journal*, pp. 24-37, 1994.

